Synthesis, crystal structure and crystal packing of diaza[5]helicenes†

Cristina Bazzini,[a] Tullio Caronna,[a] Francesca Fontana,[a] Piero Macchi,*[b] Andrea Mele,[cd] Isabella Natali Sora,[a] Walter Panzeri[d] and Angelo Sironi[b]

Received (in Montpellier, France) 7th January 2008, Accepted 2nd May 2008
First published as an Advance Article on the web 4th July 2008
DOI: 10.1039/b800050f

Analysis of the crystalline packing of known aza[5]helicenes is presented together with some newly synthesized diaza[5]helicenes species, characterized by NMR spectroscopy and X-ray diffraction. The comparison with carbo[5]helicenes and monoaza[5]helicenes emphasizes the importance of the "shape factor" (responsible of the *isomorphism* between some species in the series) as well as the lack of a unique supramolecular effect organizing the molecules in the crystals (responsible for the *polymorphism* observed for some compounds).

Introduction

The unusual optical, electronic and chelating properties of helicenes have renewed an interest in these molecules, characterised by helical structure and a high specific optical rotation of the separated enantiomers. In particular, nitrogen-substituted helicenes are a class of molecules with prospective application in fields such as light-emitting devices, chemosensors, dyes and data storage.[1] Compounds with potential applications for light emitting devices are the aza[5]helicenes, helical π-electron systems made of five fused carbocyclic and heterocyclic aromatic rings, where one or more nitrogen atoms substitute carbons into the structure (Fig. 1(a) provides a scheme of the framework numbering). Photoluminescence time-resolved measurements showed that the characteristic triplet lifetimes of 4-aza[5]helicene, 5-aza[5]helicene and 6-aza[5]helicene are extremely long (up to 2.4 s), and almost independent on the position of the nitrogen atom in the helicene framework.[1,2] On the other hand, the chiroptical properties of monoaza[5]helicenes—characterised by large circular dichroism (CD) effects, large optical rotation values and rates of racemisation—show a marked dependence on the position of the nitrogen atom in the helicene molecule.[3]

Here, we report on a general synthetic route we used to prepare a series of diaza[5]helicenes and on their structural properties. The products 4,11-diaza[5]helicene (**1**) and 5,10-diaza[5]helicene (**2**) were prepared, as described in a preceding work,[2] by photochemical cyclization of the corresponding di(quinolyl)ethene, obtained by reacting a quinolinecarbaldehyde with a (quinolylmethyl)triphenylphosphonium chloride. 1,7-diaza[5]helicene (**3**) and 1,12-diaza[5]helicene (**4**) were prepared instead by photochemical cyclization of the corresponding pyridinylbenzoisoquinolylethene, obtained by reacting a benzoisoquinoline carbaldehyde with a (pyridinylmethyl)triphenylphosphonium chloride (Scheme 1).

We have determined, by X-ray single crystal diffraction, the crystal structures of some members of the families of symmetric (namely **1** and **2**) and asymmetric (**3** and **4**) diaza[5]helicenes. Our investigation was carried out also with the purpose of rationalizing the packing of these molecules in the crystalline state. Coupling the information of diaza[5]helicenes with those previously obtained on monoaza[5]helicenes,[2] we could appreciate the variety of motifs characteristic of these species and rationalize their tendency toward *isomorphism* (*i.e.* similar spatial arrangements of different molecules) as well as toward *polymorphism* (*i.e.* different arrangements of the same molecule).

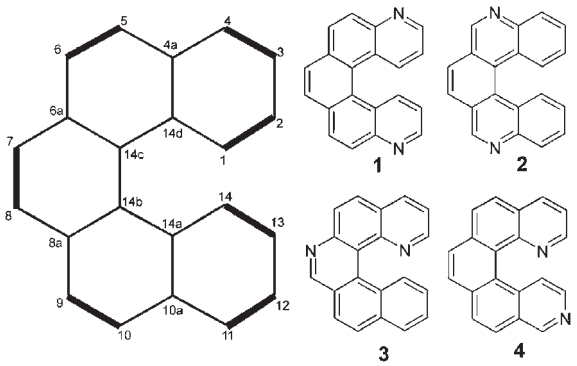

Fig. 1 Left: Schematic structure of [5]helicene and labelling of the sites available for the heteroatoms. C–C bonds having shorter distances in the parent carbo[5]helicene are drawn with bold lines. Right: The diaza[5]helicenes (**1–4**) described in this work.

[a] *Dipartimento di Ingegneria Industriale Università di Bergamo viale Marconi 5, 24044 Dalmine, Italy*
[b] *Dipartimento di Chimica Strutturale e Stereochimica Inorganica, Università degli Studi di Milano, via Venezian 21, 20133 Milano, Italy. E-mail: piero.macchi@unimi.it*
[c] *Dipartimento di Chimica, Materiali e Ingegneria Chimica G.Natta, Politecnico di Milano, via L. Mancinelli 7, 20131 Milano, Italy*
[d] *CNR – Istituto di Chimica del Riconoscimento Molecolare, via L. Mancinelli 7, 20131 Milano, Italy*

† Electronic supplementary information (ESI) available: Table S1 containing crystallographic details and Scheme S1 illustrating structures of compounds **8–14**. Crystallographic information files for species **1**, **2-I**, **2-II**, **2-III**, **3**, **4** (the same labelling is used in the block data of the CIF). CCDC reference numbers 686815–686820. For ESI and crystallographic data in CIF or other electronic format see DOI: 10.1039/b800050f

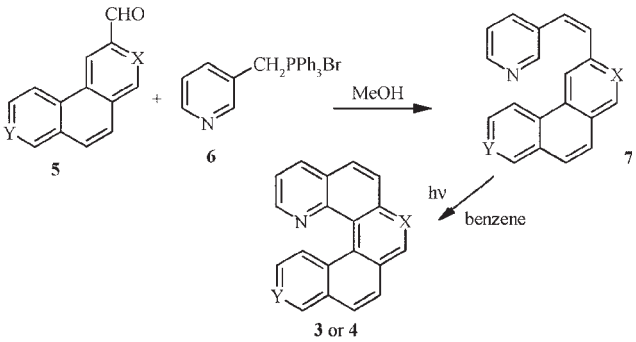

5a: X = N, Y = C Benzo[f]isoquinoline-2-carbaldehyde
5b: X = C, Y = N Benzo[h]isoquinoline-9-carbaldehyde
7a: X = N, Y = C 2-(2-pyridin-3-yl-vinyl)-benzo[f]isoquinoline
7b: X = C, Y = N 9-(2-pyridin-3-yl-vinyl)-benzo[f]isoquinoline

Scheme 1

Experimental

Synthesis

The details of the synthesis and characterization of the symmetrical 4,11-diaza[5]helicene (**1**) and 5,10-diaza[5]helicene (**2**) have been described elsewhere.[2,4] The three polymorphic crystalline forms of **2** were obtained after slow evaporation at room temperature using CH_2Cl_2, $CHCl_3$ and ethyl acetate as re-crystallization solvents for **2-I**, **2-II** and **2-III**, respectively. The synthetic route to achieve preparation of 1,7- and 1,12-diaza[5]helicenes (**3**) and (**4**) is based on the general strategy followed in a previous paper[1] (Scheme 1). The vinyl derivative (**7**) is prepared through a Wittig reaction from the appropriate aldehyde (**5**) and the phosphonium salt (**6**), and is then cyclized photochemically to the desired diazahelicene (**3–4**). The precursors **5a**, **5b** and **6** were prepared as described in ref. 1 and in the references cited therein.

General procedure—All the starting materials were commercial products and were used without further purification. NMR spectra were performed on Bruker Avance 500 spectrometer operating at proton resonance frequency of 500 MHz. The products were dissolved in $CDCl_3$ and tetramethylsilane (TMS) was added as internal reference. NOE experiments were carried out by using standard library pulse sequences. GC-MS analyses were obtained from an Agilent GC 6890 series gas-chromatograph equipped with a MS 5973N mass spectrometer detector. Electrospray mass spectra (ESI-MS) were acquired on a Bruker Esquire 3000+ by infusion of suitable solution directly in the ESI source (rate 4 μl min^{-1}).

Wittig reactions—In a typical procedure, MeONa (0.065 g, 1.5 mmol) was added under stirring to a mixture of 1 mmol of the aldehyde (**5a,b**) and 1 mmol of (pyridin-3-ylmethyl)triphenylphosphonium bromide (**6**) in 15 mL methanol. The mixture was gently boiled for 4 h. After cooling, water was added and the solution extracted many times with a large volume of CH_2Cl_2. After drying and removal of the solvent the residue was purified by flash chromatography on silica gel with ethyl acetate–hexane (3 : 2) eluting mixture, obtaining, respectively **7a,b** in the form of a mixture of *cis* and *trans* isomers, which on standing, probably due to the effect of light, slowly turns into the pure *trans* isomer.

Photochemical reactions—The vinyl derivative (**7**) (1 mmol) was dissolved in benzene in a vessel open to the air. The vessel was irradiated with visible or UV light monitoring the advancement of the reaction in time by GC, and stopping irradiation when most of the precursor had disappeared and/or byproducts began to appear. The solvent was removed under vacuum and the residue was chromatographed on silica gel, yielding **3** or **4**, respectively.

2-(2-Pyridin-3-yl-vinyl)benzo[*f*]isoquinoline (7a). 1a was reacted as indicated in the general procedure. Yield 90%, mp 60–62 °C, ESI-MS m/z 283 $[M + H]^+$, ^1H NMR ($CDCl_3$) Signals belonging to the pyridyl moiety are labelled as "py": δ 9.27 (1H, br s, H4), 8.91 (1H, d, J = 2.3 Hz, H1py), 8.76–8.73 (1H, m, H10), 8.56 (1H, dd, J = 1.7 and 4.8 Hz, H5py), 8.48 (1H, s, H1), 7.99–7.96 (1H, m, H7), 7.89 (1H, A part of AB system, J = 16.0 Hz, proton on double bond), 7.86 (2H, m, H5+H6), 7.76 (1H, ddd, J = 1.7, 2.3 and 8.0 Hz, H3py), 7.72–7.67 (2H, m, H8+H9), 7.51 (1H, B part of AB system, J = 16.0 Hz, proton on double bond), 7.36 (1H, dd, J = 8.0 and 4.8 Hz, H4py).

1,7-Diaza[5]helicene (3). 80 mg of **7a** were dissolved in 200 mL of benzene and photolyzed at 350 nm overnight. The crude product was chromatographed on silica gel with a ethyl acetate–hexane (5 : 1) eluting mixture; yield 62%. **3** has mp 220–223 °C, ESI-MS m/z 281 $[M + H]^+$, ^1H NMR ($CDCl_3$) δ 9.43 (1H, br s, H8), 8.77 (1H, dd, J = 1.9 and 4.2 Hz, H2), 8.41 (1H, dd, J = 1.3 and 8.6 Hz, H14), 8.34 (1H, dd, J = 1.9 and 8.2 Hz, H4), 8.29 (1H, d, J = 8.8, H6), 8.09 (1H, d, J = 8.6 Hz, H10), 8.07 (1H, d, J = 8.8 Hz, H5), 7.99 (1H, dd, J = 1.6 and 8.2 Hz, H11), 7.98 (1H, d, J = 8.6 Hz, H9), 7.67 (1H, ddd, J = 1.3, 6.9 and 8.2 Hz, H12), 7.48 (1H, dd, J = 4.2 and 8.2 Hz, H3), 7.38 (1H, ddd, J = 1.6, 6.9, 8.6 Hz, H13).

9-(2-Pyridin-3-yl-vinyl)benzo[*f*]isoquinoline (7b). 5b was reacted as indicated in the general procedure. Yield 83%, MS m/z 282 ($M^+ + 1$, 40%), ^1H NMR matches the spectrum reported in the literature.[5]

1,12-Diaza[5]helicene (4). 120 mg of **7b** were dissolved in 100 mL of benzene and photolyzed with visible light for 1 week. The crude product was chromatographed on silica gel with ethyl acetate as the eluent; some precursor is left unreacted and two products are formed, **4** (R_f 0.27, yield 15%) and 1,14-diaza[5]helicene (R_f 0.21, yield 70%). **4** has mp 160–165 °C, ESI-MS m/z 281 $[M + H]^+$, ^1H NMR: ($CDCl_3$) 9.33 (1H, s, H11), 8.74 (1H, dd, J = 1.9 and 4.2 Hz, H2), 8.38 (1H, d, J = 6.1 Hz, H13), 8.31 (1H, dd, J = 8.2 and 1.9 Hz, H4), 8.05 (1H, dd, J = 8.6 and 1.0 Hz, H10), 8.01 (1H, d, J = 8.6, H6), 8.02–7.97 (3H, m, H7 + H8 + H9) 7.95 (1H, ddd, J = 1.0, 1.0 and 6.1, H14), 7.94 (1H, d, J = 8.6, H5), 7.55 (1H, dd, J = 4.2 and 8.2 Hz, H3).

X-Ray diffraction

All crystals were mounted on a glass fiber in air and collected at room temperature on a Bruker SMART CCD (**3**, **2-I**, **2-II**, **2-III**) and Bruker SMART-APEX CCD (**1**, **4**). Crystal data are reported as ESI† (Table S1). Graphite-monochromatized

Mo-Kα (λ = 0.71073 Å) radiation was used with the generator working at 45 kV and 40 mA (SMART) or 50 kV and 30 mA (SMART-APEX). Orientation matrixes were initially obtained from least-squares refinement on *ca.* 300 reflections measured in three different ω regions, in the range $0 < \theta < 23^\circ$; cell parameters were optimised on the position, determined after integration, of all reflections above 10 $\sigma(I)$ level. The intensity data were collected in the full sphere (with ω scan method) within $2\theta < 64^\circ$ for **2-I**, **2-II** and **2-III** and within $2\theta < 47^\circ$ for **1**, **3** and **4** (whose diffraction was significantly smaller). An empirical correction for diffraction anisotropies was applied to raw data (SADABS).[6] Details of the data collections are given in ESI† (Table S1).

The structures were solved by direct methods (SIR97)[7] and refined with full-matrix least squares (SHELX97)[8] on F^2 on the basis of independent reflection; anisotropic temperature factors were assigned to all non-hydrogenic atoms. Hydrogens were riding on their carbon atoms, though whenever possible, they have been freely refined. Location of N atoms were assumed based on the absence of peaks at expected position of a bonded H atom and by the reduced skeletal bond distances. However, all the X-ray geometries show smaller gaps between C–C and C–N pseudo-equivalent distances compared to DFT optimizations suggesting the possible presence of some disorder about the molecular pseudo-twofold axis, which was actually observed for the asymmetric species **3** and **4**. Details of the crystal structure refinement are given in ESI† (Table S1).

Theoretical calculations

Geometry optimization and electron density calculations were carried out at B3LYP/6-31G(d,p) level of theory using the program GAUSSIAN03.[9] Molecular volumes were computed based on 0.001 e bohr^{-3} density envelope for all molecules. However, a more consistent estimation of the molecular volumes was obtained using van der Waals spheres (used to compute the packing coefficients reported in Table 1). Electrostatic interaction energies were obtained from the total molecular densities of each pair under study with the program SPDFG;[10] repulsive and dispersive interaction energies were computed using Williams and Cox parameters.[11] Hirshfeld surfaces and fingerprints were produced with the program Crystal Explorer.[12] Plots of the crystalline packing were produced with Mercury.[13]

Results and discussion

Synthesis and NMR characterization

The synthesis was obtained through the usual protocol, by photochemical cyclization of the corresponding vinyl derivative (**7**), obtained by a Wittig reaction between aldehydes **5a,b** and the phosphonium salt **6**; these precursors were all prepared as described in ref. 1. The products **7** were mixtures of the *cis* and *trans* isomers which, on standing, slowly turned into the pure *trans* isomer, which was then characterized. Upon irradiation with UV light, the *trans* isomer isomerizes to *cis*, which then cyclizes.

The characterization of the products was carried out by NMR and electrospray ionization mass spectrometry (ESI-MS). The full assignment of the NMR spectra was obtained by the combined use of selective decoupling and steady-state ^{1}H{^{1}H} NOE difference spectra or COSY and NOESY two-dimensional techniques, as previously shown.[2] Interestingly, compound **4** exhibits a long-range coupling constant ^5J between H10 and H14 *via* a W pathway for spin–spin coupling, as previously reported[1] for 3-aza- and 7-aza[5]helicenes.

Structural characterization

We studied the molecular structures of diaza-helicenes in order to establish possible relationships between chemical bonding features and molecular properties of these molecules. For this reason, we report on the X-ray structure determination of some members of the families of symmetric and asymmetric diaza[5]helicenes, namely 4,11-diaza[5]helicene (**1**), 5,10-diaza[5]helicene (**2**), 1,7-diaza[5]helicene (**3**) and 1,12-diaza[5]-helicene (**4**). Previously, we have reported on the structures of some monoaza[5]helicenes (**10–12**), whereas structural information is available in the literature for carbo[5]helicene (**8**)[14,15] and 1,14-diaza[5]helicene (**14**).[5] 1-aza[5]helicene (**9**) and 7-aza[5]helicene (**13**) have been determined in our laboratories

Table 1 Summary of the known monoaza, diaza and carbo[5]helicenes. V_{mol} is the van der Waals (v.d.W.) volume of the gas phase molecule; V is the unit cell volume, Z is the number of molecules in the unit cell; the packing coefficient is the ratio between the volume occupied by v.d.W. atomic spheres and the unit cell volume; I.R. is the *isomorphic relationship* with other crystalline structures determined in this Table; μ is the computed molecular dipole moment. For sake of clarity standard settings of the space groups are reported (whereas in the original literature non-standard settings might have been reported); Unpubl. = unpublished work.

[5]Helicene	Label	Space group	V_{mol}/Å^3	(V/Z)/Å^3	Packing coeff.	I.R.	μ/D	Ref.
Carbo	**8a-I**	$C2/c$	265	365	0.704	**10**	0.1	14, 15
	8a-II	$P2_1/c$		359	0.718	—		15
1-Aza	**9**	$C2/c$	260	346	0.728	**14**	1.7	Unpubl.
4-Aza	**10**	$C2/c$	260	358	0.698	**8a-I**	2.3	2
5-Aza	**11**	$P2_1nb$	259	355	0.703	—	2.6	2
6-Aza	**12**	$P2_1/c$	260	354	0.715	**3**, **13**	2.2	2
7-Aza	**13**	$P2_1/c$	260	348	0.724	**12**, **3**	2.4	Unpubl.
1,7-Diaza	**3**	$P2_1/c$	256	343	0.718	**12**, **13**	2.0	This work
1,12-Diaza	**4**	$P2_1/c$	255	339	0.725	—	4.2	This work
1,14-Diaza	**14**	$C2/c$	257	337	0.738	**9**	0.3	5
4,11-Diaza	**1**	$Pbca$	254	343	0.735	—	0.5	This work
5,10-Diaza	**2-I**	$P2_1/c$		343	0.724	—		This work
	2-II	$C2/c$	254	349	0.705	—	0.3	This work
	2-III	$Pbcn$		338	0.737	—		This work

but are yet unpublished (see Table 1 for a summary of all available structural data and labelling scheme).

We can therefore discuss on the molecular geometries of these species as well as on their arrangements at supramolecular level with the aim to explore the main trends observed in the solid state.

At molecular level, the main structural feature is of course the helical shape, which implies a *true* (as in the symmetric diaza-) or a *pseudo* (as in the asymmetric diaza- and monoaza-) twofold axis bisecting the bonds between atoms 7, 8 and 14b, 14c (see Fig. 1 for labelling). In crystals of asymmetric molecules, disorder is often encountered about the pseudo-twofold axis.

In Table 1, the packing efficiency is also reported. For each molecule, we calculated the optimised molecular geometry at B3LYP/6-31G(d,p) level (in agreement with our previous study)[2] and then the molecular volume (estimated *via* the volume of van der Waals spheres). Notably, the gas-phase molecular volume does not depend much on the position of the heteroatom. In fact, carbo[5]helicene (**8**) has a molecular volume around 265 $Å^3$, monoaza[5]helicenes have volumes around 260 $Å^3$ and diaza[5]helicenes around 255 $Å^3$. As a result, the packing efficiency reported in Table 1 seems to correlate more with the type of packing than with the type of molecules. For example, the most efficient packing is that of 1,14-diaza[5]helicene (**14**) and its isomorphous 1-aza[5]helicene (**9**), whereas the least efficient one is that of carbo[5]helicene in *C*2/*c* form (**8a-I**) and its isomorphous 4-aza[5]helicene (**10**). A similar trend is verified if we consider the molecular geometries refined from X-ray diffraction data. In this case, however, the molecular volumes are more variable and they slightly correlate with the observed torsion about the central ring (evaluated from torsion about 14b–14c bond). This parameter might substantially differ from the theoretical gas-phase predictions, suggesting that it is somewhat affected by the molecular packing (though we should take into account the large uncertainties associated with the experimental values). On the other hand, the small modification produced by a different torsion of the molecule is not enough to substantially change the packing efficiency of a given crystalline arrangement.

In Table 2, a selection of intramolecular bond distances is reported. Of course, for those crystals where structural disorder was observed, the accuracy of the molecular geometry is lower, though in general sufficient to draw some conclusion.

The molecular geometry of the helicene skeleton contains alternation of short and long C–C bonds (see Fig. 1). The longer bonds are those mostly affected by the intramolecular torsion (namely 14a–14b, 14b–14c and 14c–14d), usually above 1.45 Å. The insertion of one or two heteroatoms produces a perturbation, however, as previously reported for monoaza[5]helicenes, this is generally limited to the first carbon neighbours and does not affect the alternation of short and long bonds in the aromatic rings. In addition we cannot register any molecular change that could be imputed to different crystalline environments (as shown, for example, by the small standard deviation from the mean of compounds **2**, known in three different polymorphs, one of which having two independent molecules in the asymmetric unit).

Analysis of the packing motifs of helicenes

At the supramolecular level, one might be driven to think that the helical nature of the molecules induces an acentric packing or at least an acentric assembling in the first coordination sphere. However, almost all crystalline species we investigated are centrosymmetric. The most frequent molecular self recognition motifs are reminiscent of the typical packing of aromatic rings:

Motif **(a)**: the anti-parallel stacking between *central* aromatic rings (as occurring in all species **2**, in **8a-I** and **10**, see Fig. 2);

Motif **(b)**: the parallel "pseudo stacking" between the two *lateral* rings (as in **3**, **4**, **12** and **13**, see Fig. 3);

Motif **(c)**: the anti-parallel stacking between the *lateral* rings (as in **1**, **8a-I**, **10**, **9** and **14**, Fig. 4).

As described by Gavezzotti,[16] the stacking of two aromatic rings is mainly stabilized by dispersive energies and only in minor part by the electrostatic and polarization interactions. The larger size of the [5]helicenes and the presence of heteroatoms make the analysis more complicated because this is subject to even smaller energy terms. Anyway, interaction energies calculated for several helicene dimers (see Table 3) confirm that also for carbo- and aza-helicenes the stacking is mainly due to dispersive interactions, with minor contribution from the electrostatic term.

In species **2**, the two planes of the central rings—packed according to motif **(a)**—are *ca.* 3.5–3.6 Å apart, which is within the range usually observed for polyaromatic compounds. This motif implies a centrosymmetric supramolecular synthon and therefore a centrosymmetric solid state form. There are, however, several ways to pack this synthon, hence a bunch of possible centrosymmetric arrangements. One notable example is produced by 5,10-diaza[5]helicene (**2**), found in three different polymorphs. In **2-I**, some C–H groups of the two stacked helicenes (red molecules in Fig. 5(a)) point toward C═C and C–H bonds of nearby molecules or are involved in C–H···N contacts. In Fig. 5(a), five types of next nearest molecules are identified for one of the two independent molecules and three for the other. Interestingly, one set of neighbours seems to be a subset of the other. In **2-II**, the helicenes are piled on top of each other producing columns of stacked molecules (in red in Fig. 5(b)) interconnected through C–H···N contacts. In **2-III**, C–H groups of the external rings points towards aromatic rings of four neighbour molecules (Fig. 5(c)), but no contact at the N is observed. Different molecular packing can be easily compared by means of the Hirshfeld surface analysis introduced by Spackman and coworkers.[17] Fig. 7 shows the Hirshfeld surfaces and corresponding "fingerprints" for each molecule **2** in each crystalline packing (note that **2-I** has two independent molecules in the asymmetric unit). The differences described above are more clearly visible. In particular, the C–H···C═C short distances in **2-I** are those responsible of the two lateral "horns" of their fingerprints (which are somewhat similar for both independent molecules in virtue of the two similar packings they are involved in). On the other hand, these horns are slightly less pronounced in **2-II** and **2-III**.

Table 2 The main structural features for the diaza[5]helicenes characterized in this work. For compound **2**, distances are averaged over the three polymorphs. For **1** and **2**, distances are averaged over the molecular twofold symmetry, whereas for **3** and **4** data are "symmetric" because of twofold disorder. In parenthesis, we report standard deviation from the mean (or standard uncertainties, in square parenthesis, when there is no average; for **14** uncertainties are not available). Bond distances involving heteroatoms are in italics. Distances are in Å, torsions in °. Data for **8a** are computed from DFT calculations, as from ref. 2

	8a	1	2	3	4	14
1–2	1.3807	1.368(8)	1.367(4)	*1.35(2)*	*1.35(2)*	*1.319*
2–3	1.4091	1.394(3)	1.397(3)	1.378(1)	*1.38(3)*	1.403
3–4	1.3782	*1.316(3)*	1.357(5)	1.341(5)	*1.326(6)*	1.350
4–4a	1.4169	*1.362(3)*	1.406(4)	1.41(2)	1.40(2)	1.400
4a–5	1.4295	1.42(1)	*1.386(2)*	1.409(3)	1.42(2)	1.425
5–6	1.3607	1.342(2)	*1.292(5)*	1.33(1)	1.33(2)	1.338
6–6a	1.4313	1.429(7)	1.431(3)	1.444(1)	1.420(2)	1.430
6a–7	1.4237	1.416(3)	1.417(5)	*1.38(2)*	1.42(3)	1.418
7–8	1.3647	1.345[6]	1.347(1)	*1.344[6]*	1.347[6]	1.343
1–14d	1.4195	1.405(1)	1.410(4)	*1.37(2)*	1.37(5)	*1.365*
14d–14c	1.4606	1.45(1)	1.453(3)	1.450(1)	1.44(2)	1.449
14c–14b	1.4515	1.442[5]	1.444(2)	1.446[4]	1.448[5]	1.441
4a–14d	1.4311	1.41(1)	1.417(3)	1.421(2)	1.410(5)	1.413
6a–14c	1.4233	1.411(1)	1.406(4)	1.402(3)	1.40(2)	1.408
Torsion/°	29.8	30.7[5]	29(1)	26.1[5]	29.3[9]	29.3

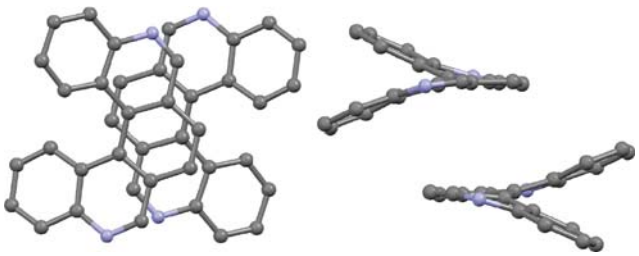

Fig. 2 Top and side view of the typical antiparallel stacking of two helicenes in **2-II**. Nitrogen atoms are in blue; hydrogen atoms are omitted.

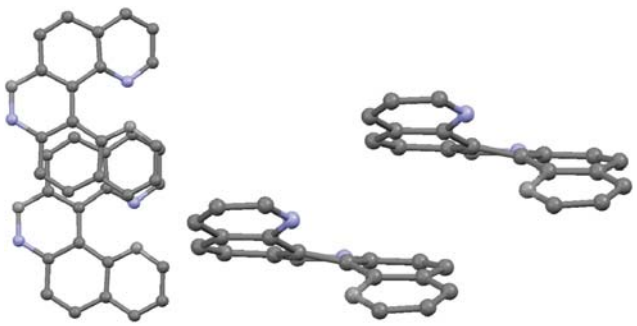

Fig. 3 Top and side view of the typical parallel "pseudo-stacking" of external rings of the two helicenes in **3**. The ring planes are actually quite diverging (as one can be appreciated by the lateral view). Nitrogen atoms are in blue; hydrogen atoms are omitted.

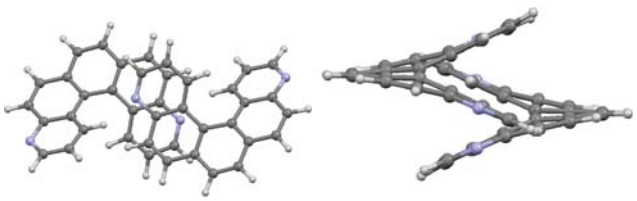

Fig. 4 Top and side view of the typical anti-parallel of external rings of the two helicenes in **1**. Nitrogen atoms are in blue.

In the "parent" [5]helicene, (**8a-I**) and in the isomorphous 4-aza[5]helicene (**10**), the same antiparallel stacking is present, but much looser than in the previous examples (the planes of the central rings are more than 3.75 Å apart, and consequently the interaction energy is smaller, see Table 3). Moreover, an alternation of motif **(a)** and **(c)** is actually present (see the sequence blue–blue–red–red in Fig. 6).

In the isomorphic species **3**, **12** and **13**, the motif **(b)** is repeated at infinite, producing columns of molecules with the same handedness (see Fig. 9). In principle this could give rise to a chiral packing, however adjacent columns assume the opposite handedness (black and red in Fig. 9) and the crystal is overall centrosymmetric. The similarity between these three species is well demonstrated by their Hirshfeld surfaces and corresponding fingerprints (see Fig. 8), although some slight differences are also visible (especially in the fingerprint plots). Notably, the interaction energies between all molecules packed with motif **(b)** are substantially identical.

In **1**, **8a-I**, **9**, **10** and **14**, motif **(c)** occurs, producing racemic columns (Fig. 10). Again most of the stabilization comes from dispersive interactions and the difference between the different species is not particularly large.

The only non-centrosymmetric crystal is that of 5-mono-aza[5]helicene (**11**), where no stacking is observed and the shortest intermolecular contacts are C–H$\cdots\pi_{(C=C)}$ (Fig. 11).

Our accurate analysis of the solid-state structures of mono- and diaza[5]helicenes shows that a strong ambiguity in the supramolecular packing exists. This is manifested in the frequent disorder of asymmetric molecules about the pseudo-twofold axis (N or C–H groups are easily interchanged), in the diffuse *polymorphisms* and in the similarly diffuse *isomorphism*. Besides, enantiomerically resolved crystalline phases have not been characterized (with the only exception of species **11**) and therefore we may expect even more (chiral) packing motifs, which are yet unknown. All these observations speak for a substantial equilibrium between the different intermolecular forces at work. For example, electrostatic forces are certainly involved, given the polarity induced by

Table 3 Decomposition of the interaction energies (in kJ mol^{-1}) between pair of molecules for the principal packing motifs in the aza[5]helicenes

Packing motif	Compound	Repulsion	Dispersion	Electrostatic	Total
Antiparallel stacking of central rings **(a)**	**2-II**	+51.4	−104.3	−10.2	−63.1
	8a-I	+26.8	−80.5	−5.5	−59.2
	10	+26.6	−79.2	−7.9	−60.5
Parallel ''pseudo-stacking'' of lateral rings **(b)**	**3**	+22.4	−66.3	−6.7	−50.6
	12	+26.4	−68.4	−7.1	−49.1
	13	+26.1	−71.3	−7.5	−52.7
	4	+20.8	−59.8	−4.7	−43.7
Antiparallel stacking of lateral rings **(c)**	**1**[a]	+20.5	−54.6	−7.4	−41.5
	9	+22.4	−62.0	−3.5	−43.1
	14	+25.8	−67.0	−11.8	−53.0
	8a-I	+22.6	−69.7	−1.1	−48.2
	10	+21.2	−64.5	−1.7	−45.0
C–H···N	**1**[b]	+16.4	−14.1	−12.9	−10.6
	2-II	+5.3	−12.0	−5.0	−11.7
	10	+3.5	−9.1	−3.4	−9.0
C–H···π	**8a-I**[c]	+5.8	−11.5	−1.3	−7.0
	11	+5.0	−19.7	−1.4	−16.1

[a] For 4,11-diaza[5]helicene, the motif **(c)** also implies two symmetric C–H···N contacts (with C···N distance of 3.667 Å). [b] C···N distance in this contact is 3.420 Å. [c] This dimer is similar to that of the isomorphic **10** which produces a C–H···N contact.

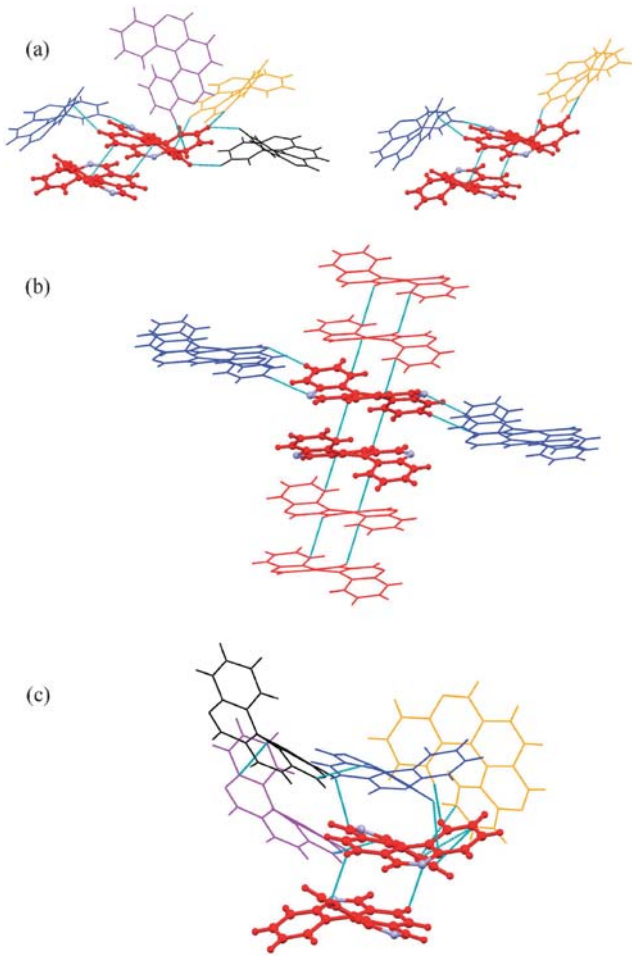

Fig. 5 Arrangements of the antiparallel stacked synthon in **2-I** (a) with two independent molecules, **2-II** (b) and **2-III** (c). The stacked molecules are ball and stick (C and H in red, N in blue). Shortest intermolecular distances are reported as cyan lines.

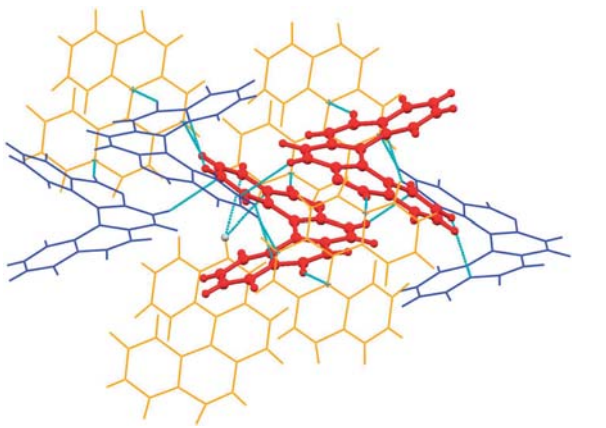

Fig. 6 Side view of the antiparallel stacking in **8a-I** and **10**. Head-to-tail and co-facial packing with surrounding helicenes are present (the former being more relevant).

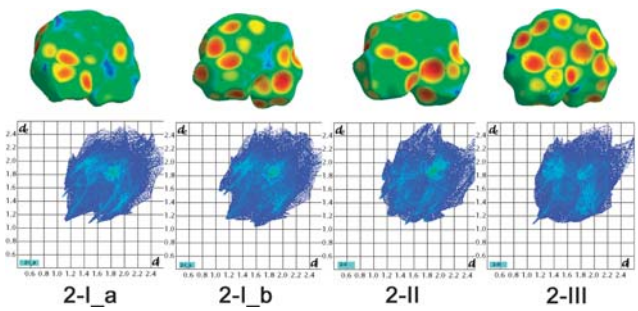

Fig. 7 Hirshfeld surfaces (top) and relative fingerprints (bottom) for molecules of species **2** in crystalline environments (**2-I** has two independent molecules in the asymmetric unit). Colour scales are the same indicated by Spackman and co-workers[17] (red colour indicates closer intermolecular distances from the surface).

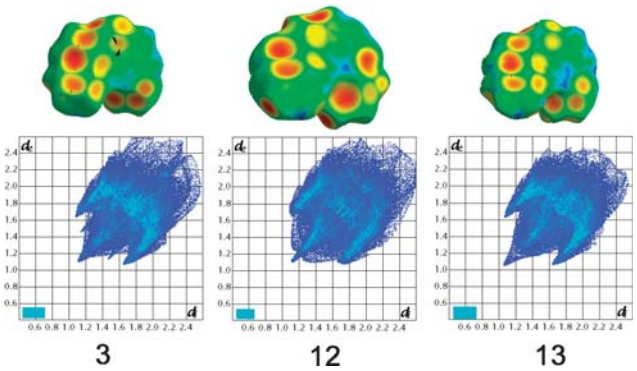

Fig. 8 Hirshfeld surfaces (top) and relative fingerprints (bottom) for molecules of species **3**, **12** and **13** which are isomorphous in the solid state.

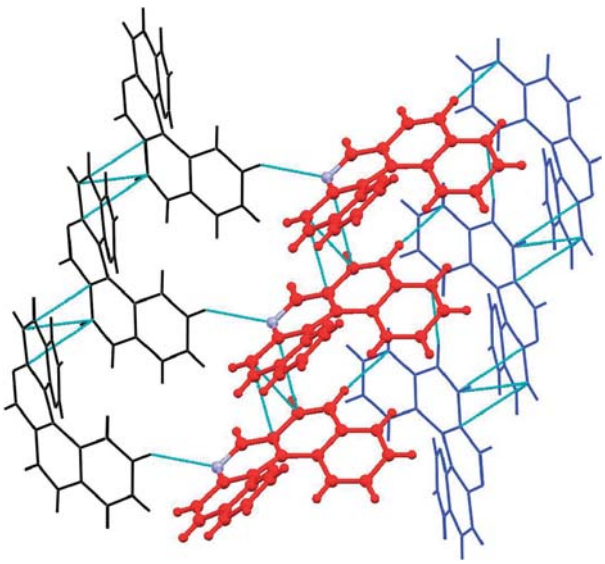

Fig. 9 A view of the columns of pseudo stacked helicenes in **3**, **12** and **13**.

one or two heteroatoms inserted at different sites of the carbo[5]helicene skeleton. As a matter of facts, the computed dipole moments are quite spread, ranging from 0.1 (for **8**) to 4.2 Debye (for **4**). However, the electrostatic interactions are not particularly important to stabilize the aggregation of two helicenes, whereas dispersive forces are always more important (see results given in Table 3). For example, the same crystalline packing is shown by carbo[5]helicene (**8a-I**) and 4-aza[5]-helicene (**10**) despite their quite different dipole moments.

For the overall stability of a given crystalline form (hence, its lattice energy), we shall not forget the important contribution of long range interactions, which have not been evaluated in this work.

Hydrogen bonding is quite modest due to the lacking of good donor groups and interactions of this kind are limited to C–H···N type (see ESI†). One interesting comparison is that between the two isomorphs **10**, having the shortest C···N distance at 3.47(3) Å, and **8a-I** (where no C–H···N is possible and the "same" contact occurs with a C···C distance of 3.97 Å). Given the additional hydrogen atom that separates

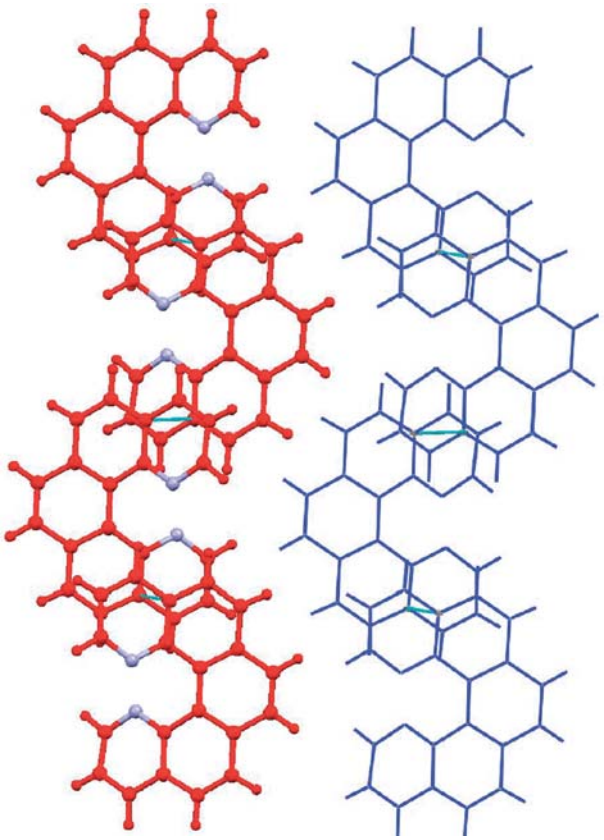

Fig. 10 The antiparallel pseudo stacking of external rings occurring in **9** and **14** and producing racemic columns.

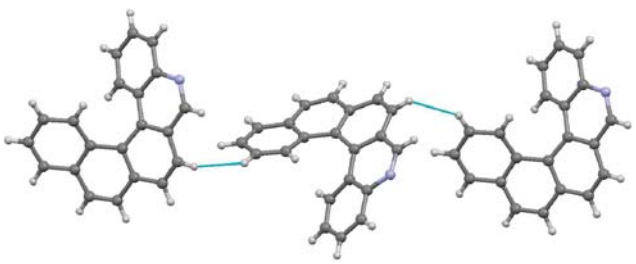

Fig. 11 The structural motif of the non-centrosymmetric crystal of species **11**.

the two carbons in this latter contact, it is quite evident that the C···N contact in **10** is hardly definable as a true weak hydrogen bond. Interaction energies also show no special differences between pairs of each species (although, the electrostatic term is more favourable for **10**, see Table 3). Another interesting comparison is that of motif **(c)** in the various species. In **1** (4,11-diaza[5]helicene), this packing actually implies also a pair of long C–H···N distances (C···N = 3.667 Å). However, this dimer is less stable than the equivalent ones formed by species **9**, **14**, **8a-I** and **10**, that instead can not have such C–H···N contact.

In other molecular packings, shortest C–H···N distances are observed, however none of these interactions is able to select one supramolecular motif against the others. Indeed a stacking implies more atom–atom interactions and usually produce a more stable pair than any "lateral" contact (as

most of the C–H···N dimers are). Due to the similar range of stabilization energies for each kind of the previously described motifs **(a)**–**(c)**, it is not surprising that *polymorphism* and *isomorphism* are equally diffuse phenomena.

Conclusions

We have examined in details the molecular geometries and crystalline packing of carbo[5]helicene and several monoaza- or diaza-heterocyclic analogous. Our purpose was to investigate those structural features responsible for physical properties which impart to these molecules a particular interest for material science. However, we observed that both at molecular and supramolecular level, the main structural features characterising carbo[5]helicene are only marginally perturbed by the heteroatom(s). For example, the position of the nitrogen(s) affects the molecular structure only "locally" (whereas charge distribution and dipole moments are more significantly modified, of course). At the same time, it seems that the shape of the helicenes, rather than the electronic or electrostatic factors, is mostly responsible of the supramolecular arrangement, given the observed attitude both towards *isomorphism* (*i.e.* same packing of different molecules) or *polymorphism* (*i.e.* different packing of the same molecule) and the frequent disorder about *pseudo*-twofold axis of the asymmetric molecules. Indeed, we cannot exclude that further research in this area could easily produce more polymorphs for all the above reported species, following the well-known statement by McCrone.[18]

References

1 S. Abbate, C. Bazzini, T. Caronna, F. Fontana, C. Gambarotti, F. Gangemi, G. Longhi, A. Mele, I. Natali Sora and W. Panzeri, *Tetrahedron*, 2006, **62**, 139.
2 C. Bazzini, S. Brovelli, T. Caronna, C. Gambarotti, M. Giannone, P. Macchi, F. Meinardi, A. Mele, W. Panzeri, F. Recupero, A. Sironi and R. Tubino, *Eur. J. Org. Chem.*, 2005, 1247.
3 F. Lebon, G. Longhi, F. Gangemi, S. Abbate, J. Priess, M. Juza, C. Bazzini, T. Caronna and A. Mele, *J. Phys. Chem. A*, 2004, **108**, 11752.
4 T. Caronna, S. Gabbiadini, A. Mele and F. Recupero, *Helv. Chim. Acta*, 2002, **85**, 1.
5 H. A. Staab, M. A. Zirnstein and C. Krieger, *Angew. Chem., Int. Ed. Engl.*, 1989, **28**, 86.
6 G. M. Sheldrick, *SADABS*, University of Göttingen, Germany, 1996.
7 A. Altomare, M. C. Burla, M. Camalli, G. L. Cascarano, C. Giacovazzo, A. Guagliardi, A. G. G. Moliterni, G. Polidori and R. Spagna, *J. Appl. Crystallogr.*, 1999, **32**, 115.
8 G. M. Sheldrick, *SHELX-97 Programs for Crystal Structure Analysis (Release 97-2)*, University of Göttingen, Germany, 1997.
9 M. J. Frisch, G. W. Trucks, H. B. Schlegel, G. E. Scuseria, M. A. Robb, J. R. Cheeseman, J. A. Montgomery, Jr., T. Vreven, K. N. Kudin, J. C. Burant, J. M. Millam, S. S. Iyengar, J. Tomasi, V. Barone, B. Mennucci, M. Cossi, G. Scalmani, N. Rega, G. A. Petersson, H. Nakatsuji, M. Hada, M. Ehara, K. Toyota, R. Fukuda, J. Hasegawa, M. Ishida, T. Nakajima, Y. Honda, O. Kitao, H. Nakai, M. Klene, X. Li, J. E. Knox, H. P. Hratchian, J. B. Cross, V. Bakken, C. Adamo, J. Jaramillo, R. Gomperts, R. E. Stratmann, O. Yazyev, A. J. Austin, R. Cammi, C. Pomelli, J. Ochterski, P. Y. Ayala, K. Morokuma, G. A. Voth, P. Salvador, J. J. Dannenberg, V. G. Zakrzewski, S. Dapprich, A. D. Daniels, M. C. Strain, O. Farkas, D. K. Malick, A. D. Rabuck, K. Raghavachari, J. B. Foresman, J. V. Ortiz, Q. Cui, A. G. Baboul, S. Clifford, J. Cioslowski, B. B. Stefanov, G. Liu, A. Liashenko, P. Piskorz, I. Komaromi, R. L. Martin, D. J. Fox, T. Keith, M. A. Al-Laham, C. Y. Peng, A. Nanayakkara, M. Challacombe, P. M. W. Gill, B. G. Johnson, W. Chen, M. W. Wong, C. Gonzalez and J. A. Pople, *GAUSSIAN 03 (Revision C.02)*, Gaussian, Inc., Wallingford, CT, 2004.
10 A. Volkov, H. F. King and P. Coppens, *J. Chem. Theory Comput.*, 2007, **3**, 232.
11 S. R. Cox, L.-Y. Hsu and D. E. Williams, *Acta Crystallogr., Sect. A*, 1981, **37**, 293.
12 S. K. Wolff, D. J. Grimwood, J. J. McKinnon, D. Jayatilaka and M. A. Spackman, *CrystalExplorer*, University of Western Australia, Perth, 2006, (http://www.theochem.uwa.edu.au/CrystalExplorer).
13 The Cambridge Crystallographic Data Center, 2007.
14 A. O. McIntosh, J. Robertson and V. Vand Monteath, *J. Chem. Soc.*, 1954, 1661.
15 R. Kuroda, *J. Chem. Soc., Perkin Trans. 2*, 1982, 789.
16 A. Gavezzotti, *CrystEngComm*, 2003, **5**, 429.
17 J. J. McKinnon, M. A. Spackman and A. S. Mitchell, *Acta Crystallogr., Sect. B*, 2005, **60**, 627.
18 W. C. McCrone, *Polymorphism in Physics and Chemistry of the Organic Solid State*, ed. D. Fox, M. M. Labes and A. Weissberger, Interscience, New York, 1965, vol. 11, pp. 726–767; J. Bernstein, *Polymorphism in Molecular Crystals*, Oxford University Press, 2002.